# Electronic Supplementary Information

# Novel cyclometalated iridium(III) phosphine-imine (P^N) complexes: highly efficient anticancer and anti- lung metastasis *in vivo*

Zhishan Xu[a, b], Yuliang Yang[b], Lihua Guo[b], Xianglei Jia[c], Lihua Guo[b], Xingxing Ge[b], Genshen Zhong[d], Shujiao Chen[b], Zhe Liu[b*]

[a] College of Chemistry, Chemistry Engineering and Materials Science, Shandong Normal University, Jinan 250014, China.

[b] Institute of Anticancer Agents Development and Theranostic Application, The Key Laboratory of Life-Organic Analysis and Key Laboratory of Pharmaceutical Intermediates and Analysis of Natural Medicine, Department of Chemistry and Chemical Engineering, Qufu Normal University, Qufu 273165, China.

[c] Henan Key Laboratory of Neural Regeneration, The First Affiliated Hospital of Xinxiang Medical University, Weihui, 453100, China.

[d] Henan Collaborative Innovation Center of Molecular Diagnosis and Laboratory Medicine, School of Laboratory Medicine, Xinxiang Medical University, Xinxiang, 453003, China.

*Corresponding author. Email: liuzheqd@163.com

## EXPERIMENTAL SECTION

**Materials.** All air-sensitive manipulations were performed under a nitrogen atmosphere. IrCl3•nH2O, 1-phenylpyrazole, 2-phenylpyridine, 2-diphenylphosphinobenzaldehyde, aniline, cyclohexylamine, 2-phenylethylamine, KPF6, DMSO and all reagents were purchased commercially and used as received unless specifically noted. All the solvents were of analytical grade. For the biological experiments, DMEM medium, fetal bovine serum, penicillin/streptomycin mixture, trypsin/EDTA, cisplatin, DAPI, MTT, and phosphate-buffered saline (PBS) were purchased from Sangon Biotech. a Phycoerythrin (PE) anti-γH2AX was purchased from Millipore. Testing compounds was dissolved in DMSO and diluted with the tissue culture medium before use. Stock solutions of cisplatin (10 mM) and complexes Ir1-Ir6 (10 mM) were prepared in PBS and DMSO, respectively. All stock solutions were stored at -20 °C, thawed and diluted with culture medium prior to each experiment.

**Animals.** All procedures involving the care and use of animals conformed to US National Institute of Health guidelines (NIH Pub. No. 85-23, revised 1996) and were approved by the laboratory animal management and experimental animal ethics committee of Department of Chemistry and Chemical Engineering, Qufu Normal University.

**NMR Spectroscopy**. $^{1}$H NMR and $^{31}$P NMR spectra were acquired in 5 mm NMR tubes at 298 K on Bruker DPX 500 (1H = 500.13 MHz) spectrometers. $^{1}$H NMR chemical shifts were internally referenced to $(CHD_2)(CD_3)SO$ (2.50 ppm) for DMSO-$d_6$, $CHCl_3$ (7.26 ppm) for chloroform-d1. All data processing was carried out using XWIN-NMR version 3.6 (Bruker UK Ltd.).

**Mass Spectra.** Mass spectra were recorded on a Atouflex Speed MALDI-TOF MS.

**Microanalysis.** Microanalysis (C, H, and N) was carried out using a Carlo Erba model EA 1108 microanalyzer.

**Synthesis of the complexes.** General Method. A mixture containing the corresponding phosphine-imine ligand (0.10 mmol), $[Ir(ppy)_2]$ $Cl_2$ or $[Ir(ppz)_2]Cl_2$ (0.05 mmol) and $CH_2Cl_2$ (20 mL) were heated 8 h at 95 ℃ under reflux in a nitrogen atmosphere. After cooling to ambient temperature, solid $KPF_6$ (0.60 mmol) was added with stirring. After, the solution was stirred for 2 h, $KPF_6$ was filtered off. The solvent was removed under reduced pressure. The crude products were purified by recrystallization using $CH_2Cl_2$/hexane or $CH_2Cl_2$/diethyl ether solution, providing yellow or white crystals, and then dried under vacuum.

**Complex Ir1** yield: 63mg (62%). $^{1}$H NMR (500 MHz, DMSO-$d_6$) δ 8.92 (s, 1H), 8.32 (d, *J* = 7.9 Hz, 1H), 8.19 (dd, *J* = 7.6, 4.3 Hz, 1H), 8.12 (d, *J* = 6.0 Hz, 1H), 8.01 (dd, *J* = 17.6, 8.9 Hz, 2H), 7.94 – 7.78 (m, 4H), 7.61 (d, *J* = 5.8 Hz, 1H), 7.57 – 7.49 (m, 2H), 7.47 – 7.32 (m, 4H), 7.26 (t, *J* = 7.5 Hz, 1H), 7.23 – 7.18 (m, 1H), 7.05 – 6.92 (m, 4H), 6.89 (t, *J* = 6.7 Hz, 1H), 6.86 – 6.73 (m, 3H), 6.26 (dd, *J* = 15.8, 7.7 Hz, 3H), 5.80 (dd, *J* = 7.3, 4.6 Hz, 1H), 3.67 – 3.56 (m, 1H), 1.80 – 1.67 (m, 2H), 1.63 (d, *J* = 13.5 Hz, 1H), 1.32 (d, *J* = 12.8 Hz, 1H), 1.19 – 1.09 (m, 2H), 0.94 (dd, *J* = 20.6, 6.7 Hz, 1H), 0.73 – 0.64 (m, 1H), 0.47 (d, *J* = 11.2 Hz, 1H), 0.16 (dd, *J* = 26.7, 13.7 Hz, 1H). $^{31}$P NMR (202 MHz, DMSO-$d_6$) δ -1.38 (s), -133.66 (s), -137.17 (s), -140.68 (s), -144.20 (s), -147.71 (s), -151.22 (s), -154.73 (s). ESI-MS (m/z): calcd for $C_{47}H_{42}IrPN_3$: 872.2746, found: 872.5. Elemental analysis calcd (%) for $C_{47}H_{42}IrN_3P_2F_6$: C, 55.51; H, 4.16; N, 4.13. Found: C, 55.62; H, 4.19; N, 4.18.

**Complex Ir2** yield: 69mg (68%). $^{1}$H NMR (500 MHz, DMSO-$d_6$) δ 9.05 (s, 1H), 8.88 (d, *J* = 5.3 Hz, 1H), 8.41 – 8.36 (m, 1H), 8.04 (t, *J* = 7.6 Hz, 1H), 7.97 (t, *J* = 7.6 Hz, 1H), 7.89 (dd, *J* = 11.7, 4.8 Hz, 2H), 7.84 (t, *J* = 6.2 Hz, 2H), 7.71 (d, *J* = 8.5 Hz, 1H), 7.62 (dd, *J* = 8.7, 7.2 Hz, 1H), 7.56 (dt, *J* = 13.2, 5.2 Hz, 3H), 7.49 – 7.41 (m, 2H), 7.35 – 7.28 (m, 2H), 7.28 – 7.24 (m, 1H), 7.15 (t, *J* = 7.4 Hz, 1H), 6.85 – 6.80 (m, 1H), 6.76 (dd, *J* = 14.0, 7.4 Hz, 3H), 6.72 – 6.63 (m, 3H), 6.61 (t, *J* = 7.2 Hz, 1H), 6.51 (t, *J* = 7.4 Hz, 1H), 6.30 – 6.20 (m, 3H), 6.08 (s, 3H), 5.46 (dd, *J* = 7.5, 4.7 Hz, 1H). $^{31}$P NMR (202 MHz, DMSO-$d_6$) δ -3.03 (s), -133.66 (s), -137.18 (s), -140.69 (s), -144.20 (s), -147.72 (s), -151.23 (s), -154.75 (s). ESI-MS (m/z): calcd for $C_{47}H_{36}IrPN_3$: 866.2276, found: 866.5. Elemental analysis calcd (%) for $C_{47}H_{36}IrN_3P_2F_6$: C, 55.84; H, 3.59; N, 4.16. Found: C, 55.95; H, 3.64; N, 4.20.

**Complex Ir3** yield: 79mg (76%). $^{1}$H NMR (500 MHz, DMSO-$d_6$) δ 8.80 (s, 1H), 8.41 (d, *J* = 8.1 Hz, 1H), 8.32 (d, *J* = 5.1 Hz, 1H), 8.09 – 8.00 (m, 2H), 7.97 – 7.87 (m, 3H), 7.84 (ddd, *J* = 19.6, 11.5, 4.8 Hz, 2H), 7.70 (d, *J* = 5.8 Hz, 1H), 7.61 – 7.56 (m, 1H), 7.55 – 7.49 (m, 1H), 7.46 – 7.33 (m, 4H), 7.23 (dd, *J* = 18.9, 8.0 Hz, 2H), 7.13 – 7.03 (m, 4H), 7.03 – 6.99 (m, 1H), 6.95 (td, *J* = 8.0, 2.4 Hz, 2H), 6.88 (t, *J* = 7.4 Hz, 1H), 6.83 – 6.73 (m, 3H), 6.39 (d, *J* = 6.3 Hz, 2H), 6.33 – 6.28 (m, 1H), 6.24 – 6.17 (m, 2H), 5.85 (dd, *J* = 7.3, 4.5 Hz, 1H), 4.04 – 3.86 (m, 2H), 2.23 (td, *J* = 11.8, 7.0 Hz, 1H), 1.90 (td, *J* = 12.0, 4.7 Hz, 1H). $^{31}$P NMR (202 MHz, DMSO-$d_6$) δ -3.15 (s), -137.17 (s), -140.68 (s), -144.20 (s), -147.71 (s), -151.23 (s), -154.74 (s). ESI-MS (m/z): calcd for $C_{49}H_{40}IrPN_3$: 894.2589, found: 894.4. Elemental analysis calcd (%) for $C_{49}H_{40}IrN_3P_2F_6$: C, 56.64; H, 3.88; N, 4.04. Found: C, 56.75; H, 3.92; N, 4.09.

**Complex Ir4** yield: 71mg (71%).$^{1}$H NMR (500 MHz, DMSO-$d_6$) δ 8.91 (d, *J* = 2.9 Hz, 1H), 8.83 (d, *J* = 2.6 Hz, 1H), 8.80 (s, 1H), 8.08 – 8.01 (m, 1H), 7.85 (t, *J* = 7.6 Hz, 1H), 7.76 (t, *J* = 7.6 Hz, 1H), 7.63 (d, *J* = 7.9 Hz, 1H), 7.51 (t, *J* = 8.0 Hz, 1H), 7.46 – 7.38 (m, 4H), 7.33 (dd, *J* = 10.7, 7.5 Hz, 2H), 7.23 (td, *J* = 8.0, 2.3 Hz, 2H), 7.01 (t, *J* = 7.1 Hz, 1H), 6.94 – 6.88 (m, 1H), 6.79 (dt, *J* = 19.3, 7.6 Hz, 2H), 6.74 – 6.64 (m, 5H), 6.40 – 6.29 (m, 2H), 6.09 (d, *J* = 7.5 Hz, 1H), 5.96 – 5.89 (m, 1H), 3.69 (t, *J* = 11.6 Hz, 1H), 1.69 (dd, *J* = 21.6, 12.5 Hz, 2H), 1.47 (d, *J* = 12.3 Hz, 1H), 1.39 (d, *J* = 9.8 Hz, 1H), 1.19 (d, *J* = 13.2 Hz, 1H), 1.14 – 1.04 (m, 1H), 1.03 – 0.83 (m, 3H), 0.44 – 0.26 (m, 2H). $^{31}$P NMR (202 MHz, DMSO-$d_6$) δ -4.17 (s), -133.66 (s), -137.17 (s), -140.68 (s), -144.19 (s), -147.71 (s), -151.22 (s). ESI-MS (m/z): calcd for $C_{43}H_{40}IrPN_5$: 850.2651, found: 850.5. Elemental analysis calcd (%) for $C_{43}H_{40}IrN_5P_2F_6$: C, 51.91; H, 4.05; N, 7.04. Found: C, 52.02; H, 4.01; N, 7.07.

**Complex Ir5** yield: 75mg (75%). $^{1}$H NMR (500 MHz, DMSO-$d_6$) δ 8.93 (s, 1H), 8.61 (d, *J* = 2.9 Hz, 1H), 8.49 (d, *J* = 2.4 Hz, 1H), 8.30 (dd, *J* = 7.1, 4.7 Hz, 1H), 8.16 (s, 1H), 7.99 (t, *J* = 7.6 Hz, 1H), 7.90 (t, *J* = 7.6 Hz, 1H), 7.71 – 7.60 (m, 3H), 7.50 – 7.43 (m, 2H), 7.40 (t, *J* = 8.4 Hz, 1H), 7.25 (t, *J* = 7.1 Hz, 1H), 7.12 (d, *J* = 7.9 Hz, 1H), 7.03 – 6.97 (m, 1H), 6.93 (td, *J* = 8.0, 2.6 Hz, 2H), 6.87 – 6.73 (m, 4H), 6.74 – 6.66 (m, 2H), 6.64 (t, *J* = 7.3 Hz, 1H), 6.62 – 6.59 (m, 1H), 6.46 (t, *J* = 7.4 Hz, 1H), 6.40 – 6.33 (m, 2H), 6.27 (d, *J* = 2.0 Hz, 1H), 6.22 (d, *J* = 6.9 Hz, 1H), 6.05 (s, 2H), 5.41 – 5.35 (m, 1H). $^{31}$P NMR (202 MHz, DMSO-$d_6$) δ -8.67 (s), -133.67, -137.18 (s), -140.69 (s), -144.20 (s), -147.71 (s), -151.23 (s), 154.74 (S). ESI-MS (m/z): calcd for $C_{43}H_{34}IrPN_5$: 844.2181, found: 844.4. Elemental analysis calcd (%) for $C_{43}H_{34}IrN_5P_2F_6$: C, 52.22; H, 3.47; N, 7.08. Found: C, 52.12; H, 3.51; N, 7.13.

**Complex Ir6** yield: 59mg (58%). $^{1}$H NMR (500 MHz, DMSO-$d_6$) δ 8.21 (d, *J* = 2.7 Hz, 1H), 8.14 (s, 1H), 7.92 (s, 1H), 7.64 (t, *J* = 7.3 Hz, 1H), 7.55 (t, *J* = 7.5 Hz, 1H), 7.44 (dd, *J* = 10.8, 8.1 Hz, 3H), 7.35 (dd, *J* = 12.2, 4.8 Hz, 3H), 7.30 (d, *J* = 7.9 Hz, 1H), 7.23 (t, *J* = 7.6 Hz, 1H), 7.15 – 6.95 (m, 8H), 6.90 – 6.80 (m, 3H), 6.77 (t, *J* = 7.5 Hz, 1H), 6.68 (t, *J* = 7.4 Hz, 1H), 6.54 (d, *J* = 2.2 Hz, 1H), 6.43 – 6.32 (m, 5H), 6.29 (d, *J* = 7.4 Hz, 1H), 6.03 – 5.96 (m, 1H), 4.16 – 4.07 (m, 1H), 4.02 (dd, *J* = 18.5, 8.8 Hz, 1H), 2.09 – 1.99 (m, 1H), 1.85 (dt, *J* = 13.2, 8.5 Hz, 1H). $^{31}$P NMR (202 MHz, DMSO-$d_6$) δ -5.94 (s), -133.65 (s), -137.16 (s), -140.67 (s), -144.19 (s), -147.70 (s), -151.21 (s). ESI-MS (m/z): calcd for $C_{45}H_{38}IrPN_5$: 872.2494, found: 872.4. Elemental analysis calcd (%) for $C_{45}H_{38}IrN_5P_2F_6$: C, 53.15; H, 3.77; N, 6.89. Found: C, 53.22; H, 3.81; N, 6.86.

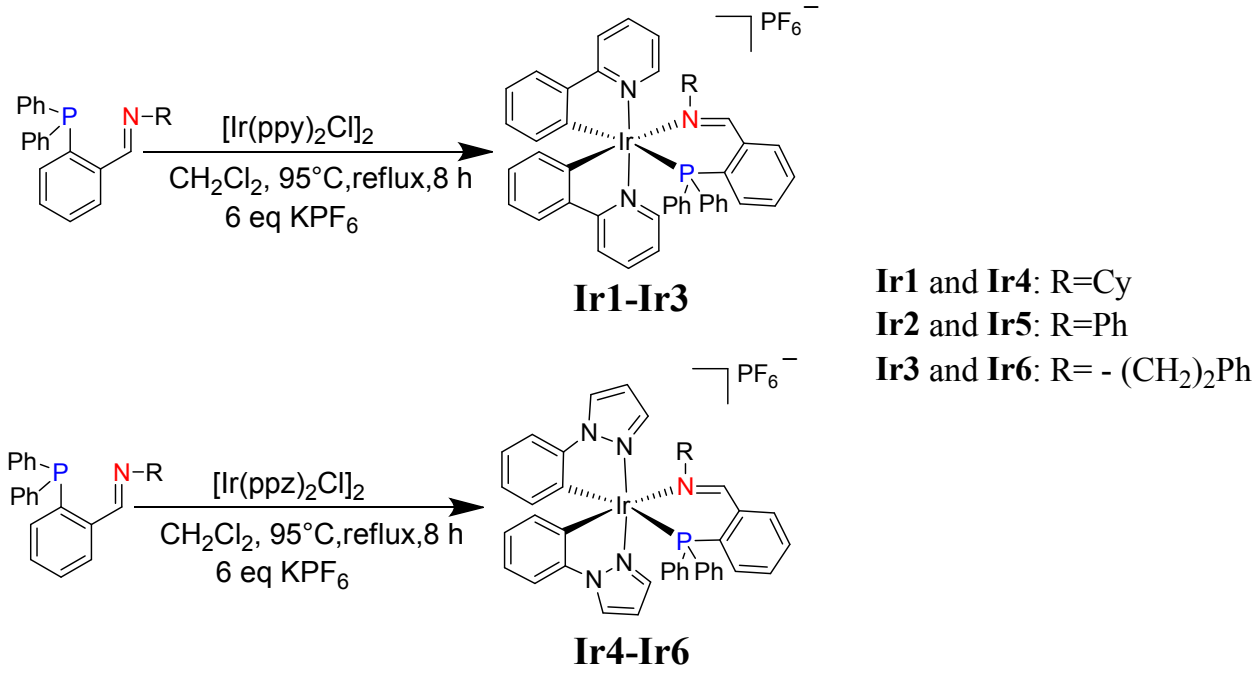


**Ir1** and **Ir4**: R=Cy
**Ir2** and **Ir5**: R=Ph
**Ir3** and **Ir6**: R= - $(CH_2)_2Ph$

**Figure S1.** Synthesis of cyclometalated iridium(III) complexes **Ir1–Ir6**.

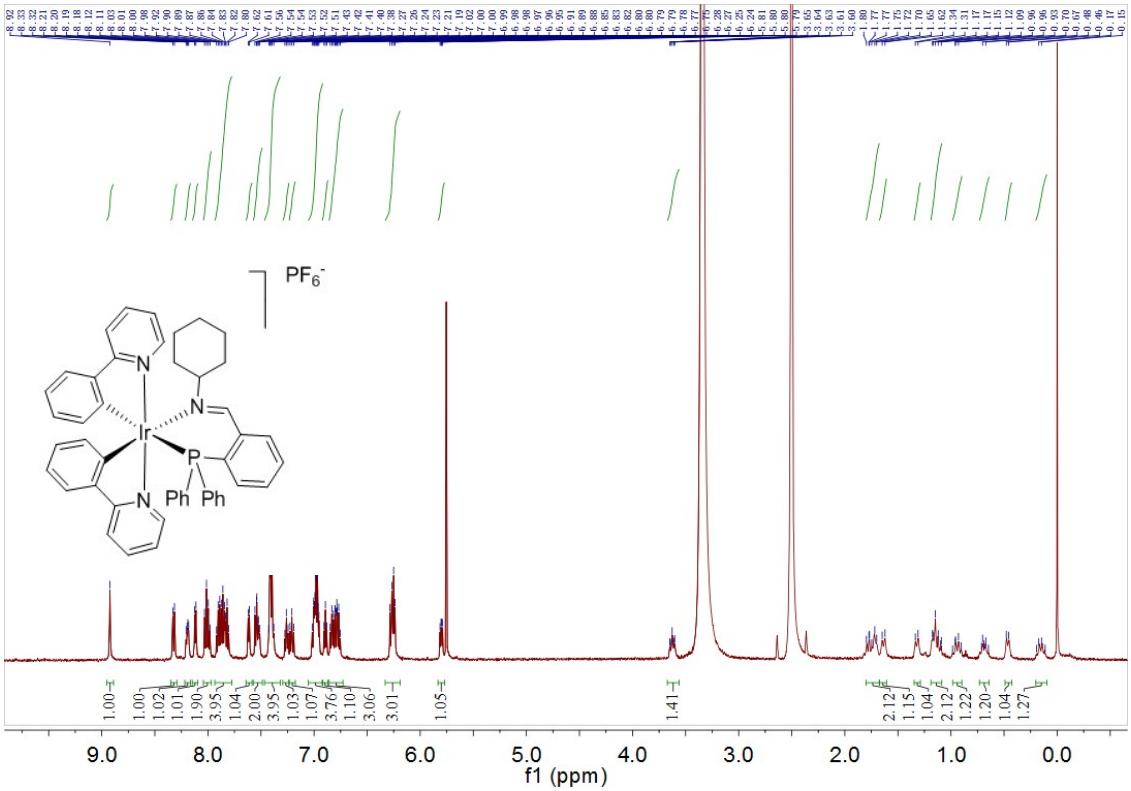


**Figure S2.** $^1$H NMR spectrum of **Ir1**.

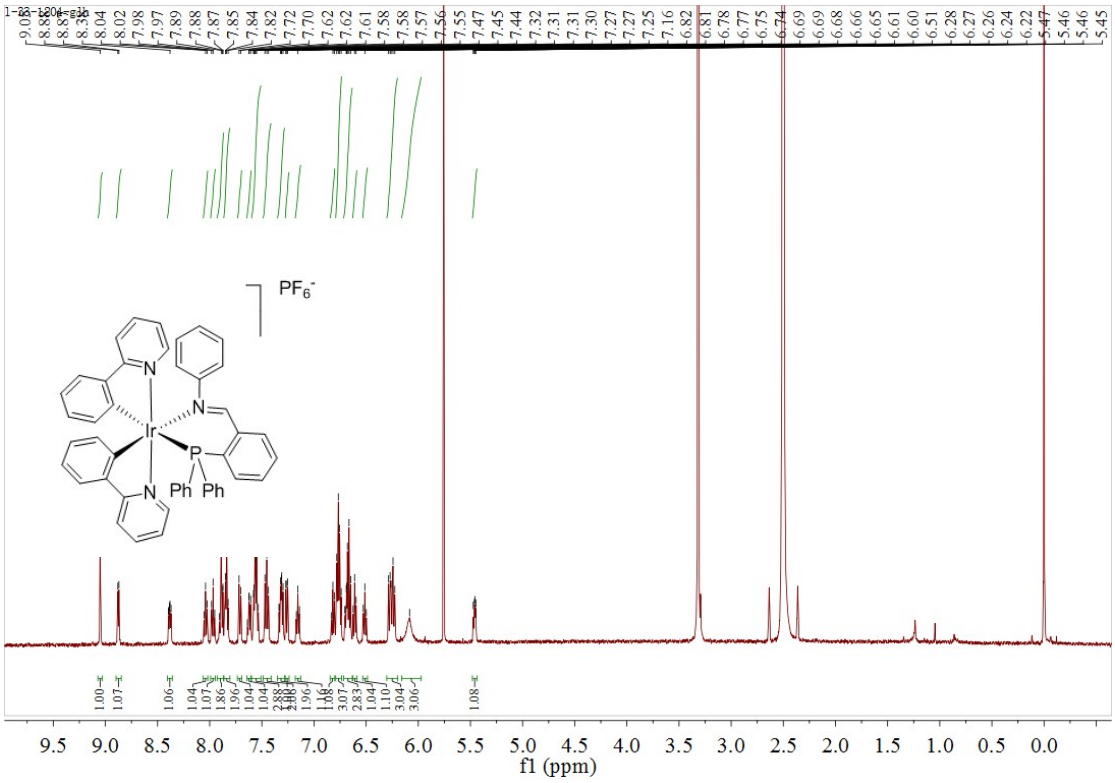


**Figure S3.** $^{1}$H NMR spectrum of **Ir2**.

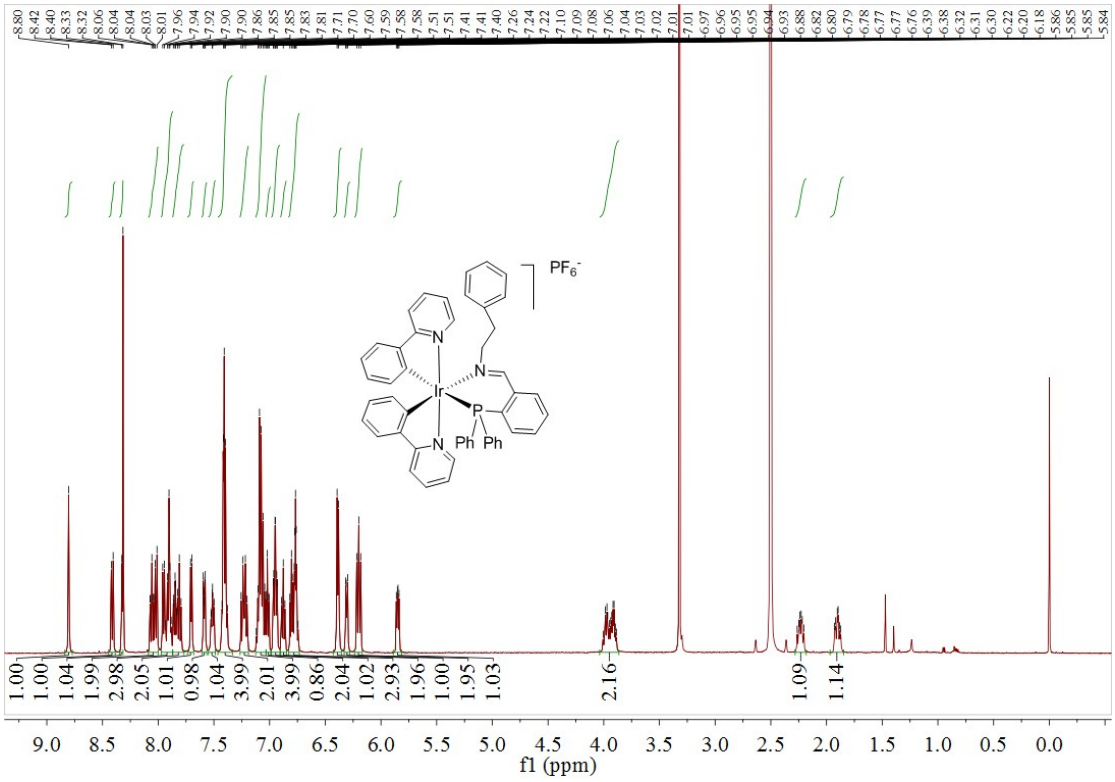


**Figure S4.** $^{1}$H NMR spectrum of **Ir3**.

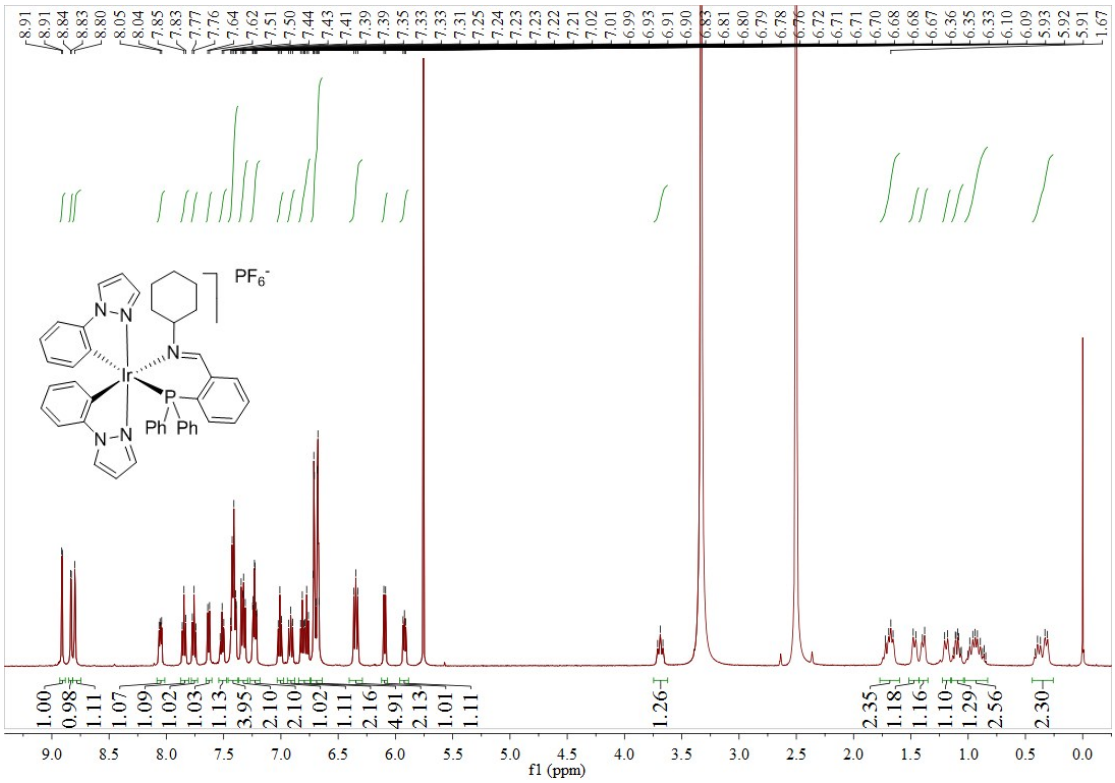


**Figure S5.** $^{1}$H NMR spectrum of **Ir4**.

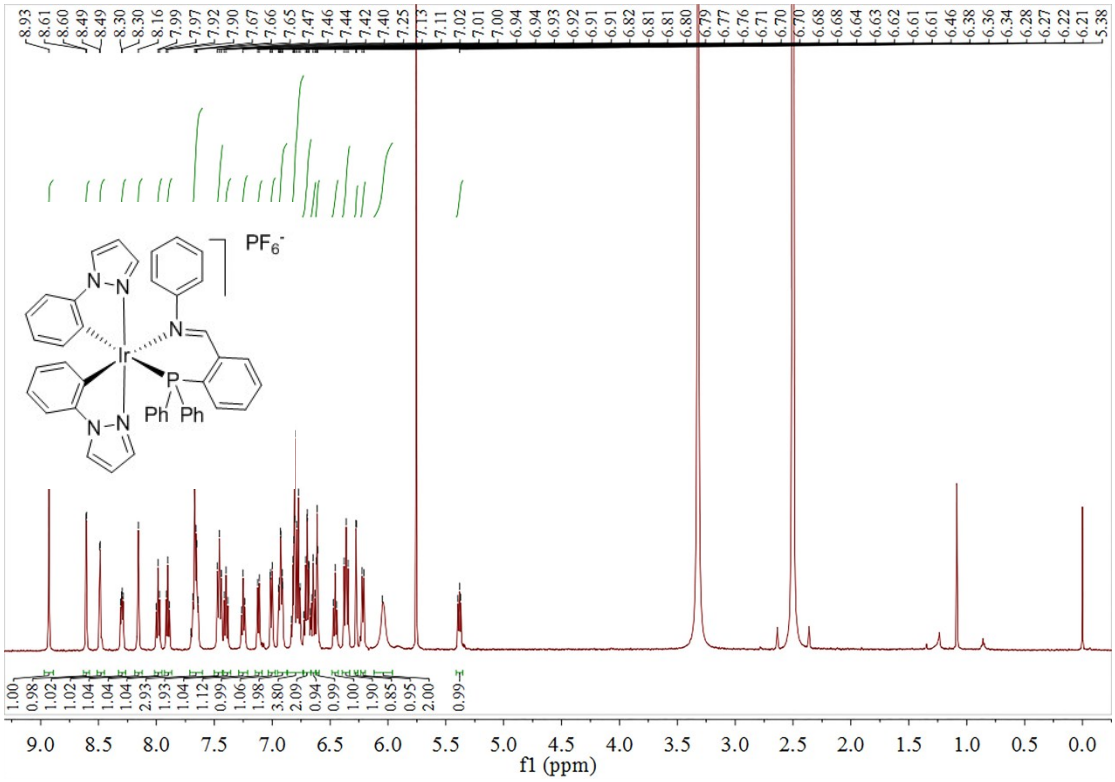


**Figure S6.** $^{1}$H NMR spectrum of **Ir5**.

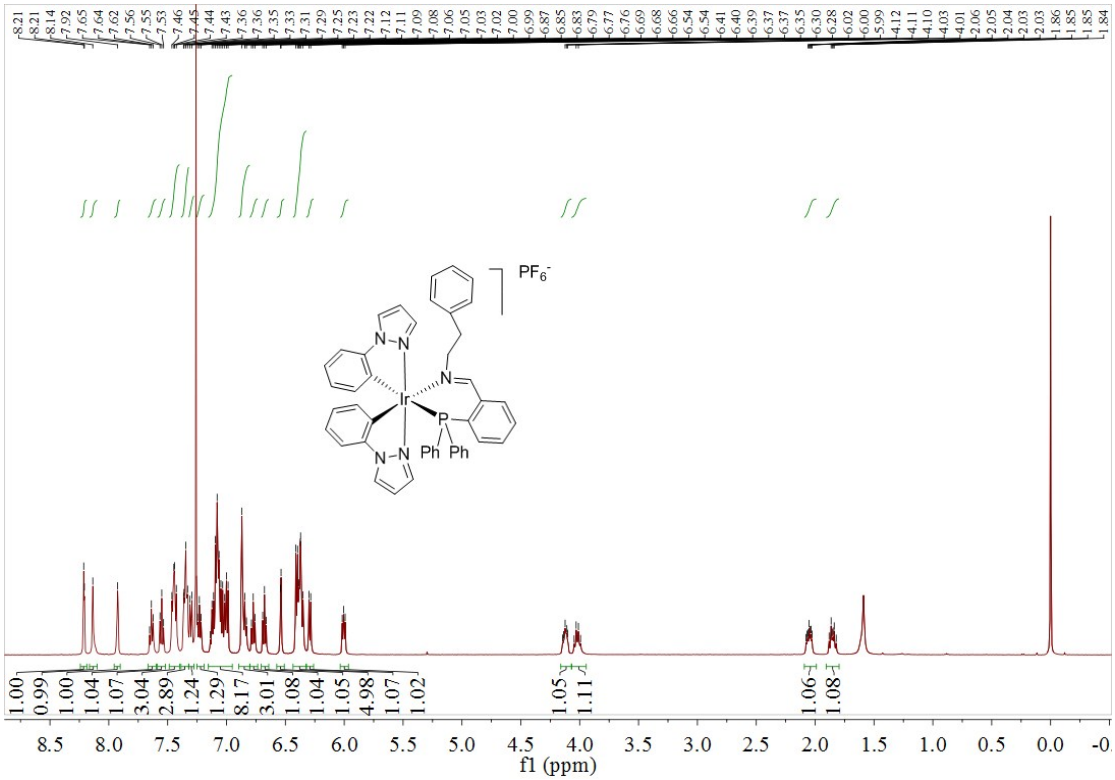


**Figure S7.** $^{1}$H NMR spectrum of **Ir6**.

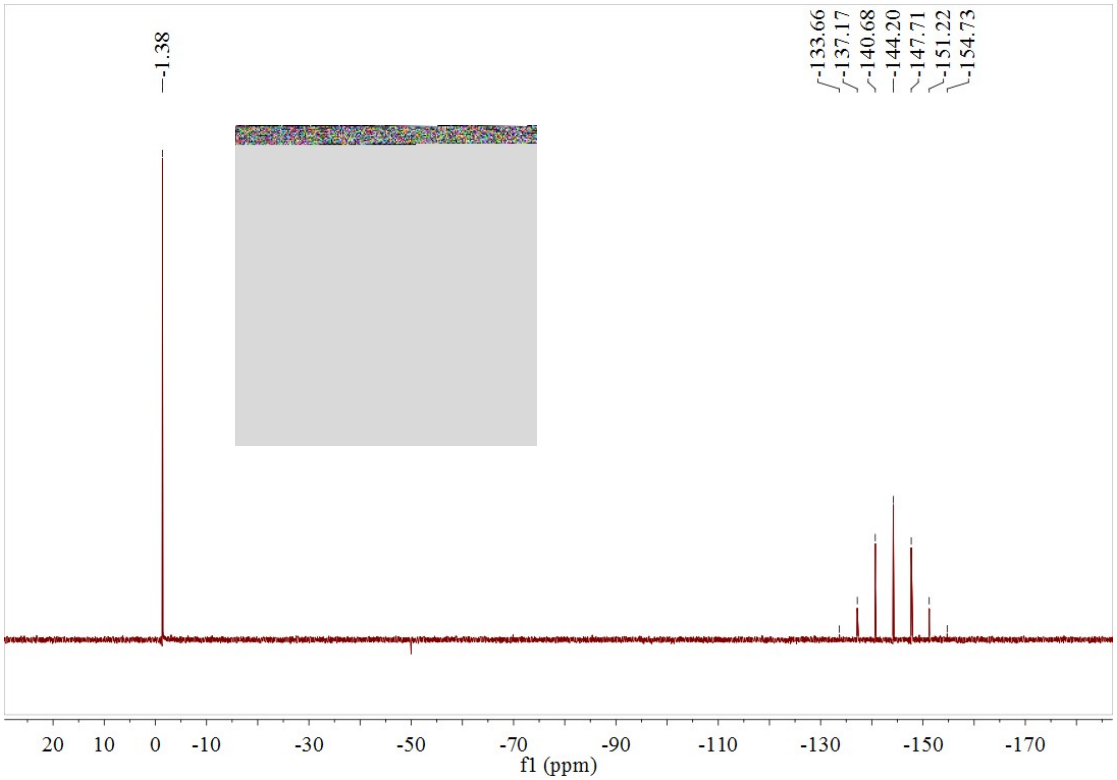


**Figure S8.** $^{31}$P spectrum of **Ir1**.

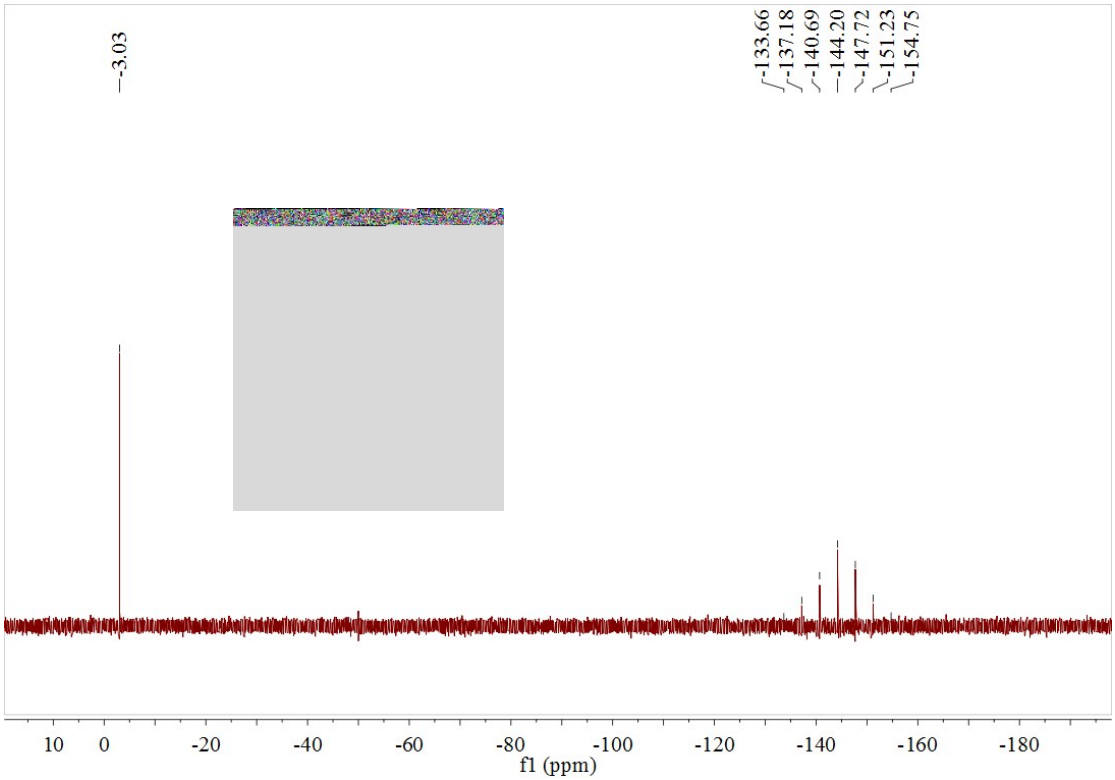


**Figure S9.** $^{31}$P spectrum of **Ir2**.

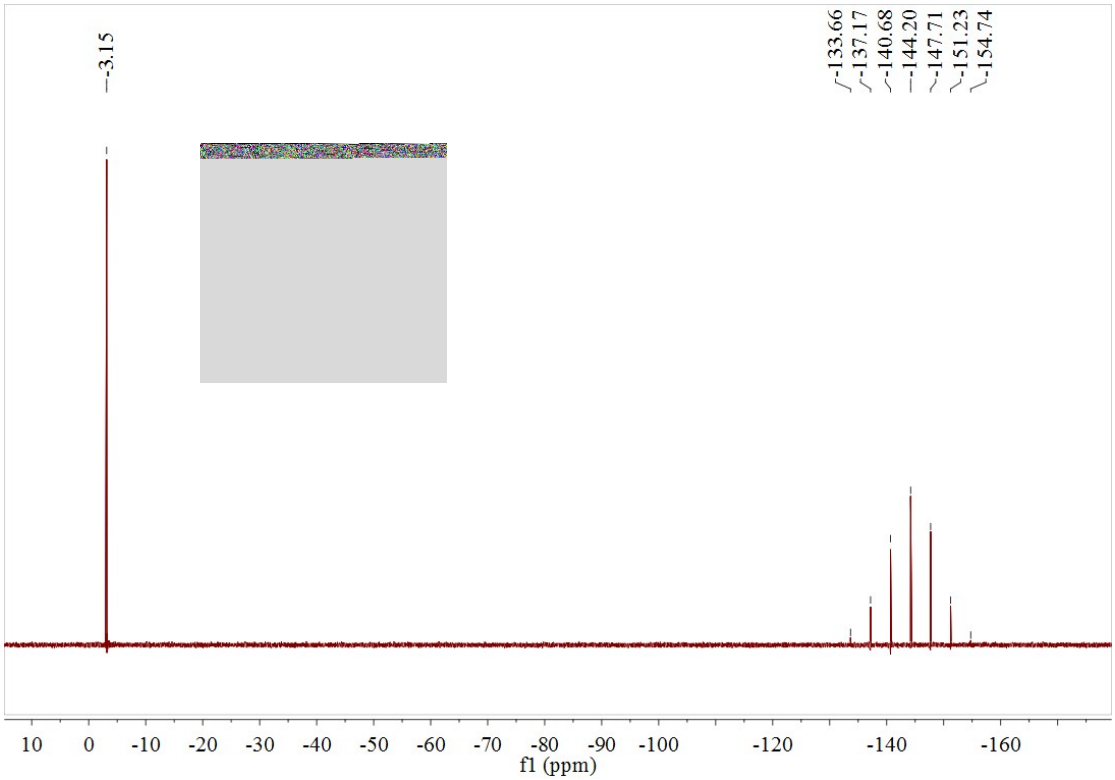


**Figure S10.** $^{31}$P spectrum of **Ir3**.

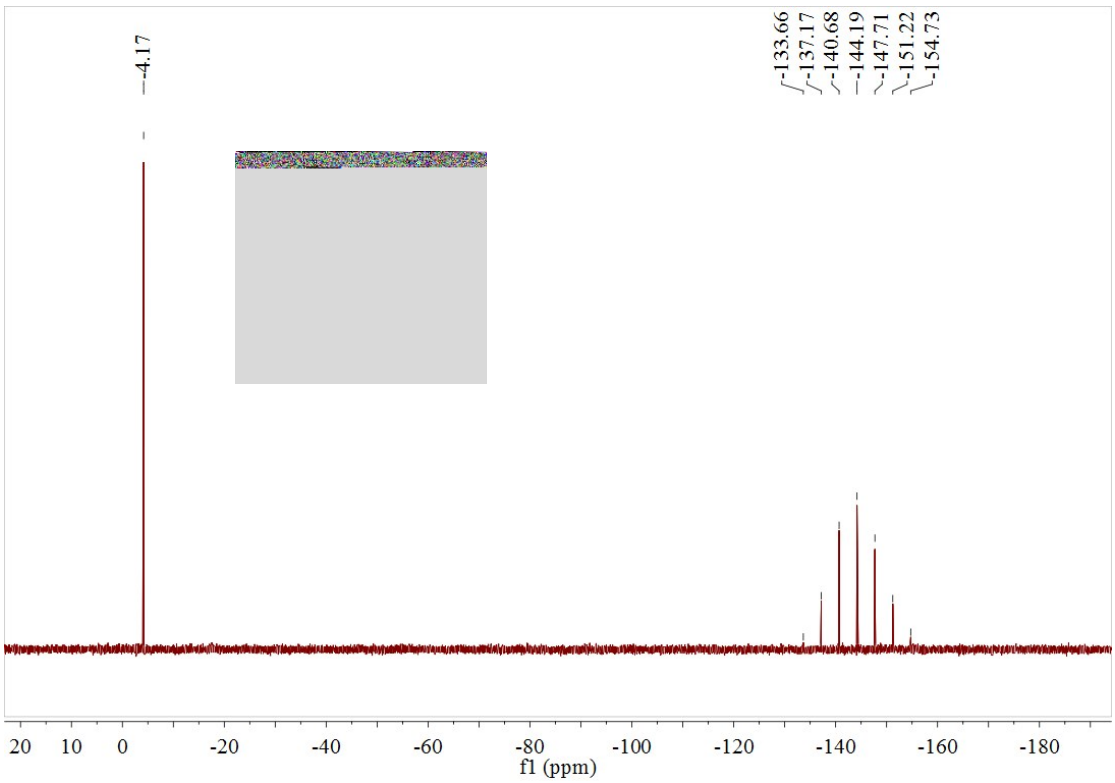


**Figure S11.** $^{31}$P spectrum of **Ir4**.

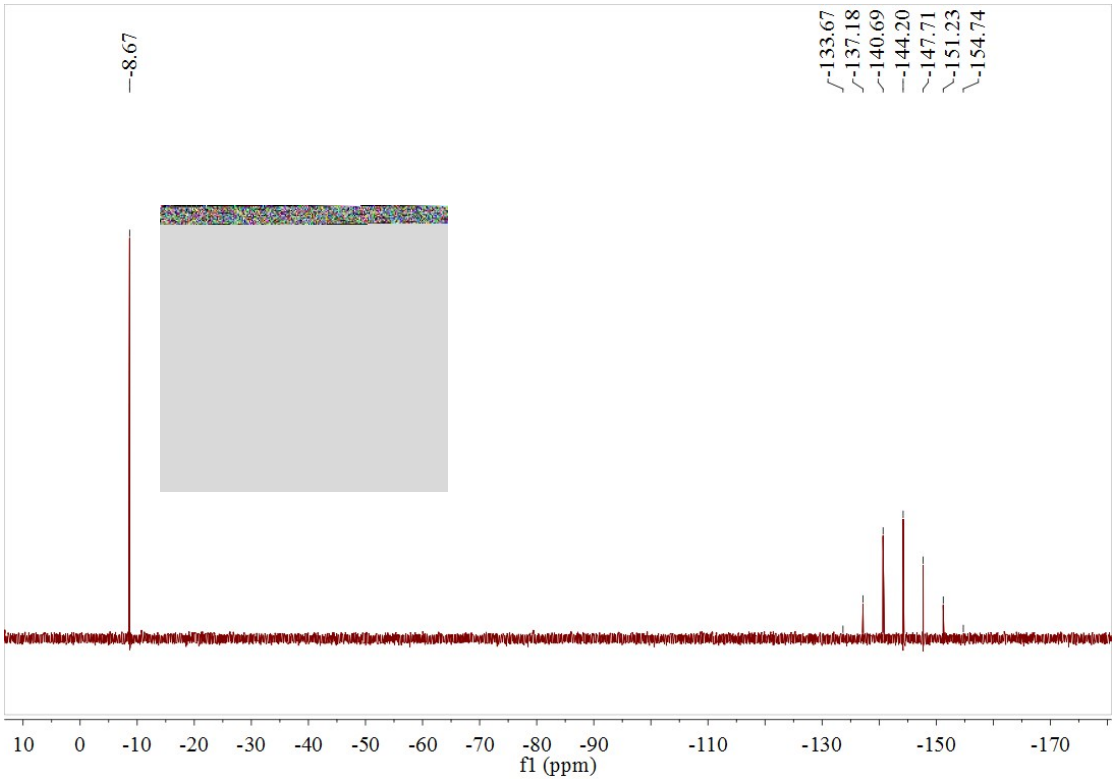


**Figure S12.** $^{31}$P spectrum of **Ir5**.

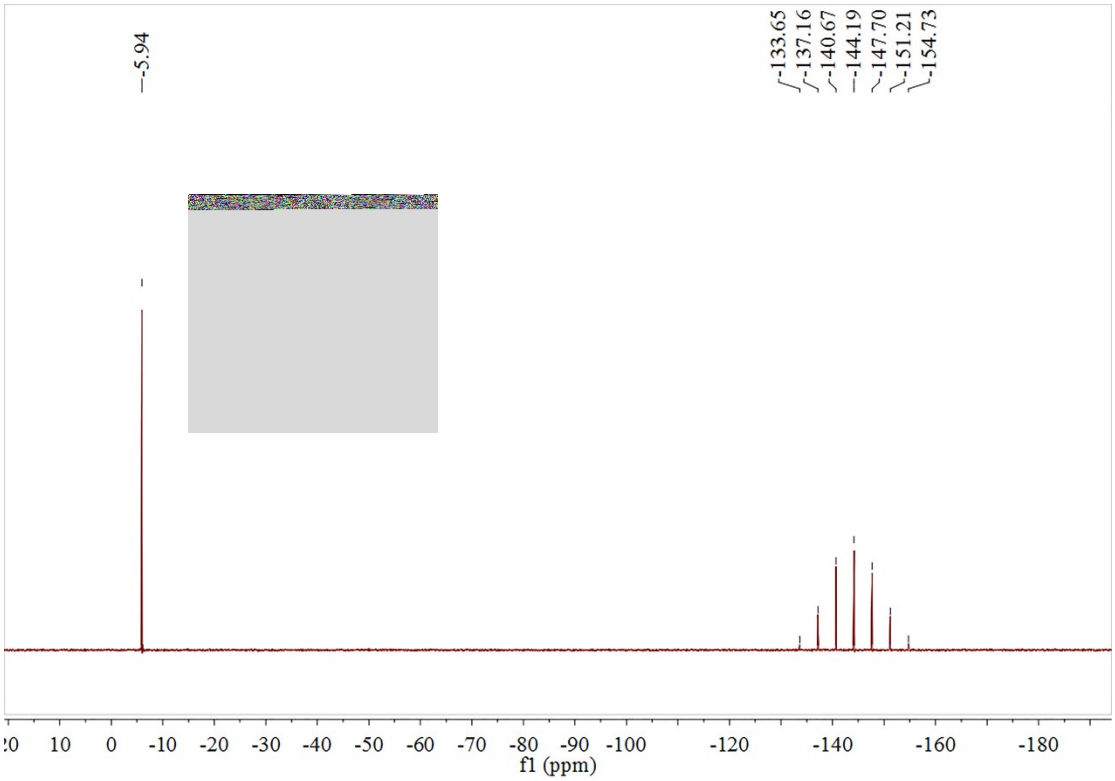


**Figure S13.** $^{31}P$ spectrum of **Ir6**.

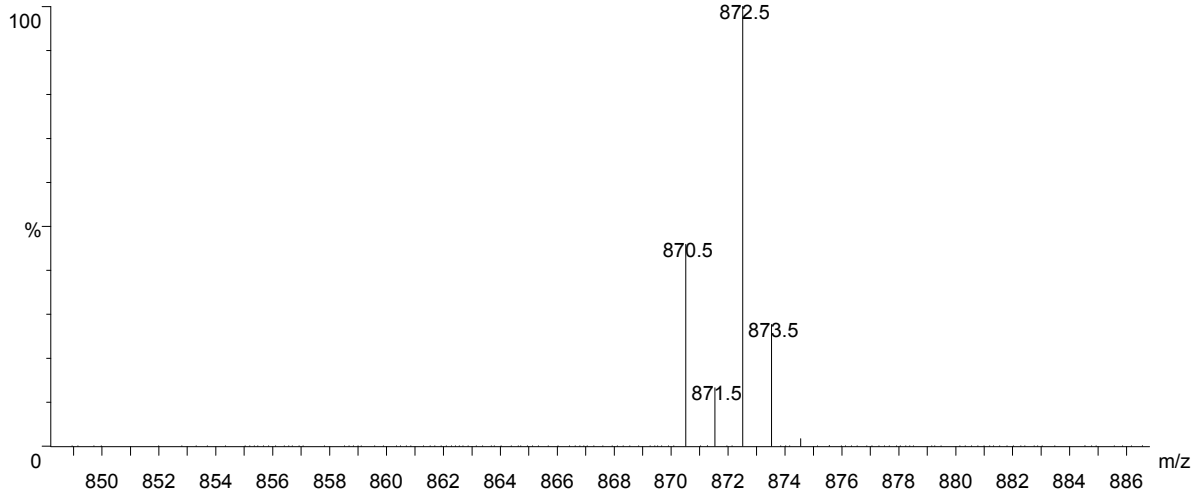


**Figure S14.** The Mass spectrometry of complex **Ir1**.

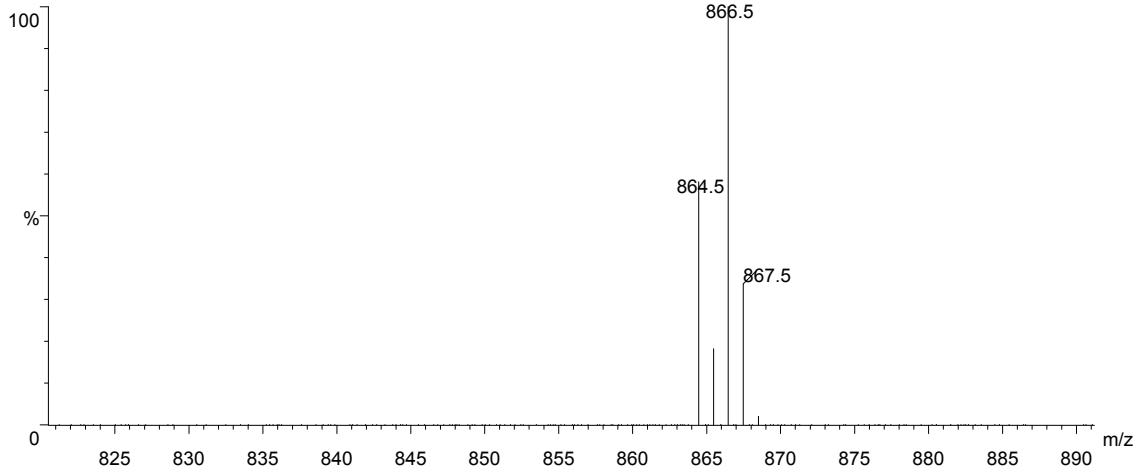


**Figure S15.** The Mass spectrometry of complex **Ir2**.

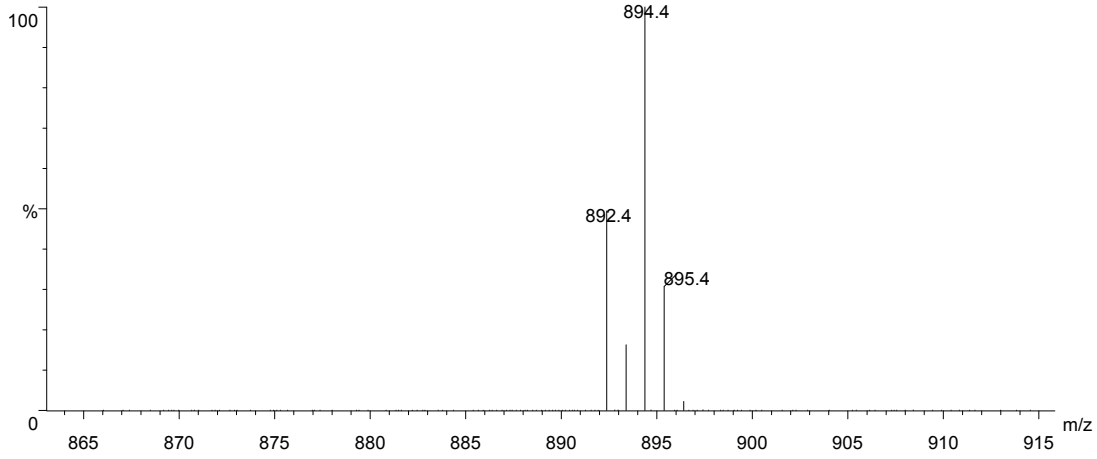


**Figure S16.** The Mass spectrometry of complex **Ir3**.

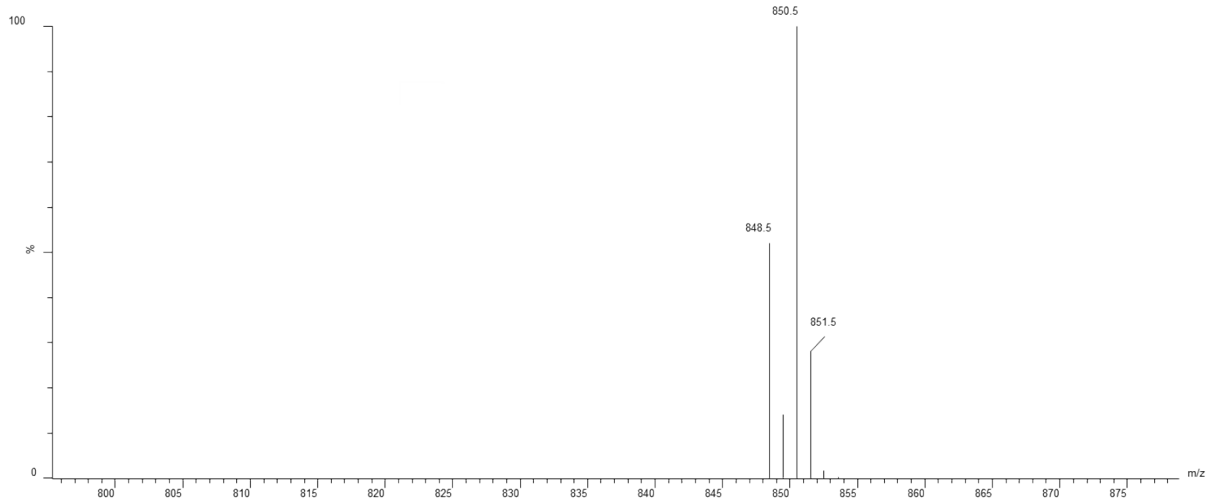


**Figure S17.** The Mass spectrometry of complex **Ir4**.

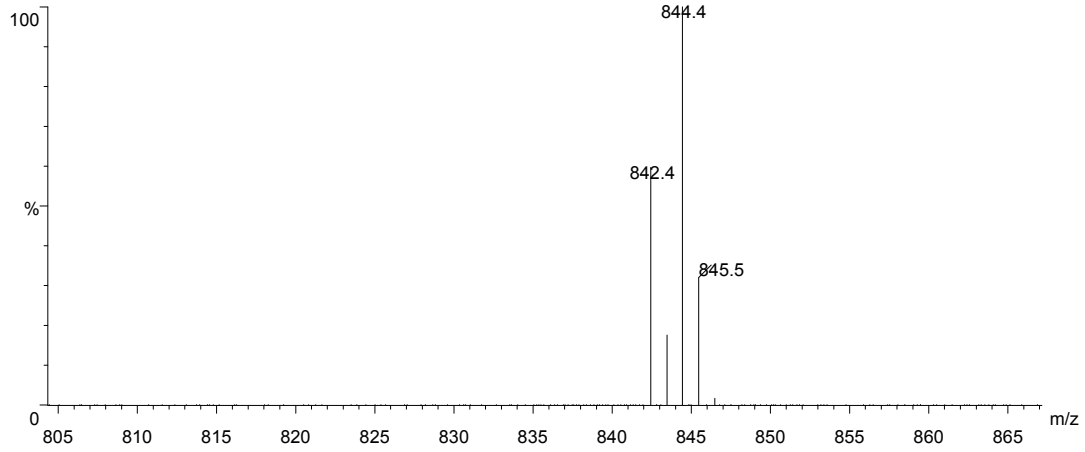


**Figure S18.** The Mass spectrometry of complex **Ir5**.

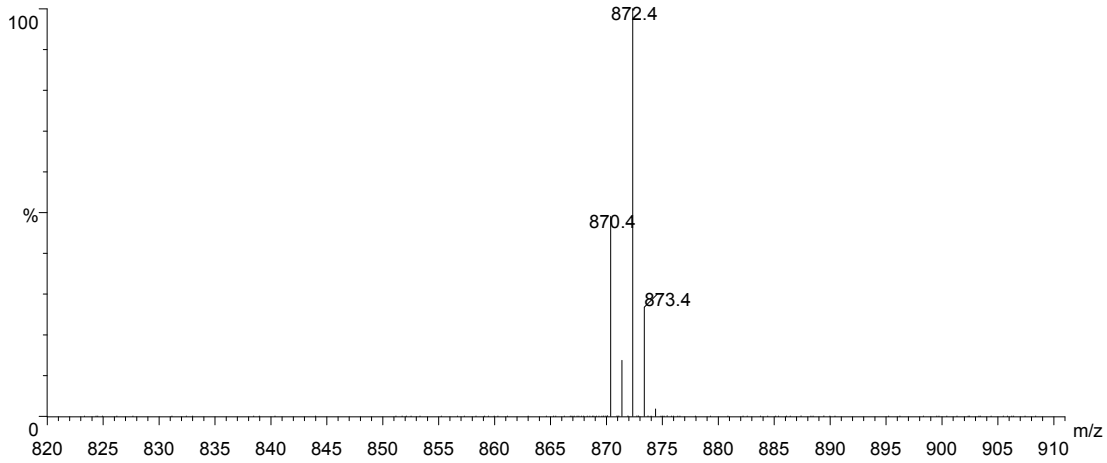


**Figure S19.** The Mass spectrometry of complex **Ir6**.

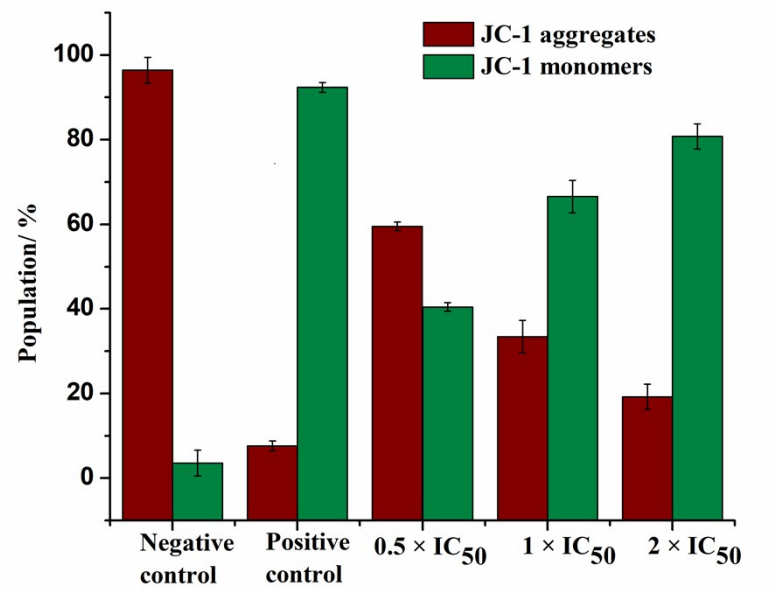


**Figure S20**. Changes in mitochondrial membrane potential of HCT116 cancer cells induced by complexes Ir3 at concentrations of 0.5 × $IC_{50}$, 1 × $IC_{50}$ and 2 × $IC_{50}$. Populations of cells that exhibit a reduction in the mitochondrial membrane potential. Data are quoted as mean ± SD of three replicates.

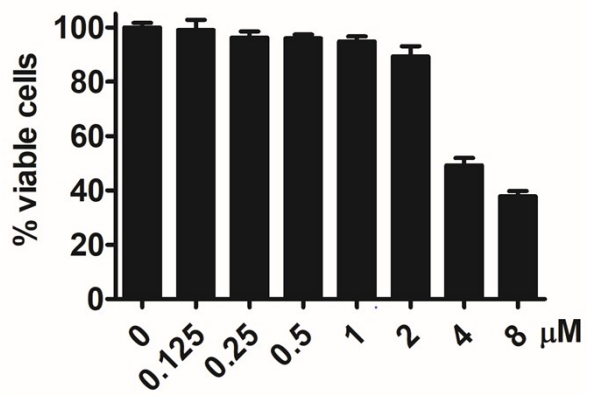


**Figure S21**. The cytotoxicity of BIX01294 towards HCT116 cancer cell after 24 h incubation.

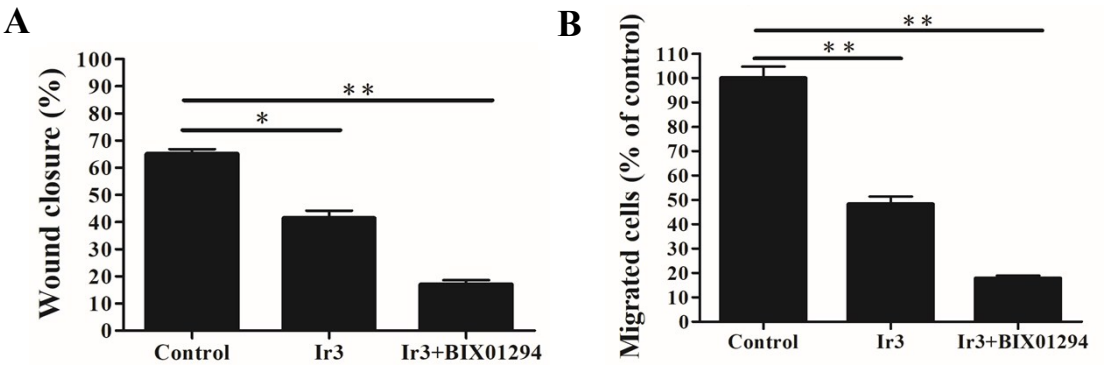


**Figure S22.** Representative graphs of migration inhibition assay. (A) For Wound-healing assay, HCT116 cells treated with complex Ir3 or the combination of Ir3 and BIX01294, typical images were taken at 0 and 24 h. Statistical data of wound-healing assay. Wound closure (%) = [1 − (distance at 24 h)/(distance at 0 h)] × 100%. (B) For migration assay, HCT116 cells treated with complex Ir3 or the combination of Ir3 and BIX01294, typical images were taken at 24 h. Statistical data of transwell invasion assay.

**Table S1**. The mitochondrial membrane polarization of HCT116 cells induced by complex **Ir3**.

| Complex | Ir concentration | Population (%) JC-1 Aggregates | JC-1 Monomers |
|---|---|---|---|
| **Ir2** | 0.5 × $IC_{50}$ | 59.5±1.0 | 40.5±1.0 |
| | 1 × $IC_{50}$ | 33.4±3.8 | 66.6±3.7 |
| | 2 × $IC_{50}$ | 19.2±3.0 | 80.8±3.1 |
| **Negative control** | | 96.4±3.1 | 3.6±3.0 |
| **Positive control** | | 7.6±1.1 | 92.4±1.2 |

**Table S2**. NAC (10 mM) reversed complex **Ir3** - elevated ROS level in HCT116 cells.

| Complex | Ir concentration | ROS ( % negative control ) |
|---|---|---|
| **Ir2** | 0.25 × $IC_{50}$ | 137.8±4.6 |
| | 0.5 × $IC_{50}$ | 155.9±5.6 |
| | 0.5 × $IC_{50}$ + NAC | 117.1±4.1 |
| **Untreated cells (Negative control)** | | 100.0±3.2 |
| **CCCP treated cells (Positive control)** | | 271.7±7.2 |

**Table S3**. Cell cycle analysis carried out by flow cytometry using PI staining after exposing HCT116 cells to complex **Ir3** or the combination of **Ir3** with **BIX01294.**

| | Population (%) | | |
|---|---|---|---|
| **Complex** | **$G_0/G_1$ phase** | **S phase** | **$G_2$/M phase** |
| **Control** | 47.7±1.3 | 35.4±0.5 | 15.4±1.4 |
| **Ir3** | 57.8±2.0 | 29.1±1.3 | 12.5±0.2 |
| **Ir3+BIX01294** | 63.9±0.8 | 24.6±3.2 | 10.9±2.0 |

**Table S4**. Flow cytometry analysis to determine the percentages of apoptotic cells, using Annexin V-PE and 7-AAD staining, after exposing HCT116 cells to complex **Ir3** or the combination of **Ir3** with **BIX01294**.

| | Population (%) | | | |
|---|---|---|---|---|
| **Complex** | **Viable** | **Early apoptosis** | **Late apoptosis** | **Non-viable** |
| **control** | 93.1±3.7 | 0.3±0.2 | 5.0±2.5 | 1.6±1.4 |
| **Ir3** | 66.7±3.6 | 0.5±0.4 | 20.5±1.4 | 12.8±2.0 |
| **Ir3+BIX01294** | 40.3±2.3 | 1.9±0.1 | 51.4±1.6 | 6.4±3.8 |

**Table S5**. Effect of **Ir3** alone or combined with **BIX01294** on lung weights and tumor nodules in BALB/c mice injected with 4T1 cells *in vivo* (n=4).

| | 4T1 cells | | | |
|---|---|---|---|---|
| | **Normal** | **Control** | **Ir3** | **Ir3+BIX01294** |
| **Lung weight (g)** | 0.13±0.01 | 0.19±0.02 | 0.16±0.02 | 0.14±0.01 |
| **Tumor nodules** | — | 211.32±27.72 | 107.52±26.01 | 29.61±8.91 |